

Targeting and tracing antigens in live cells with fluorescent nanobodies

Ulrich Rothbauer^{1,5}, Kourosh Zolghadr^{1,5}, Sergei Tillib², Danny Nowak³, Lothar Schermelleh¹, Anja Gahl³, Natalija Backmann⁴, Katja Conrath⁴, Serge Muyldermans⁴, M Cristina Cardoso³ & Heinrich Leonhardt¹

We fused the epitope-recognizing fragment of heavy-chain antibodies from *Camelidae* sp. with fluorescent proteins to generate fluorescent, antigen-binding nanobodies (chromobodies) that can be expressed in living cells. We demonstrate that chromobodies can recognize and trace antigens in different subcellular compartments throughout S phase and mitosis. Chromobodies should enable new functional studies, as potentially any antigenic structure can be targeted and traced in living cells in this fashion.

Antibodies are valuable tools for visualizing cellular components in fixed cells, but their use in living cells is limited owing to the inefficient folding and assembly of their variable heavy and light chains. So far, intracellular applications have mostly relied on direct microinjection of antibodies, which is technically demanding and stressful for cells. Fluorescent fusion proteins can easily be expressed in cells and whole organisms and provide information on protein localization and dynamics in living cells^{1,2}, but endogenous proteins, their post-translational modifications and non-protein cell components remain invisible and cannot be studied. To overcome these limitations, we fused the antigen-binding fragment of a heavy-chain antibody with fluorescent proteins. Heavy-chain antibodies³ from *Camelidae* sp. are devoid of light chains and recognize antigens via their variable domain (referred to as V_HH or nanobody; **Fig. 1a** and **Supplementary Fig. 1** online), which represents the smallest intact antigen-binding fragment⁴. On the basis of their chimeric nature, we termed these fluorescent antigen-binding nanobody fusions ‘chromobodies’.

We chose green fluorescent protein (GFP) as a first target molecule to test the feasibility of this approach. GFP has previously been fused to a variety of proteins with well-characterized subcellular localization, providing ‘visible’ antigens to directly test chromobodies in different subcellular compartments. We isolated

lymphocytes from an alpaca (*Lama pacos*) immunized with purified GFP. We amplified the coding sequence of the V_HH by PCR, cloned it into a phage display vector and identified a highly specific GFP-binding antibody fragment, α-GFP V_HH, after panning (**Supplementary Methods** online). Surface plasmon resonance measurements indicated a fast kinetic association rate of $7.68 \times 10^5 \text{ M}^{-1}\text{s}^{-1}$ and a slow dissociation rate of $1.74 \times 10^{-4} \text{ s}^{-1}$ for the interaction of α-GFP V_HH with the GFP antigen. The low dissociation constant ($K_d = 0.23 \text{ nM}$) calculated from these values was consistent with the interaction of an affinity-matured antibody recognizing its cognate antigen.

To test the distribution of α-GFP V_HH in living cells, we fused it to the monomeric red fluorescent protein (mRFP) to generate a ‘visible’ GFP-binding antibody termed the ‘GFP-chromobody’ (**Fig. 1a**). Gel filtration, immunoblotting and confocal microscopy showed that the GFP-chromobody was stable and dispersely distributed in mammalian cells and that there were no detectable signs of protein degradation (**Supplementary Fig. 2** online). We did not detect any aggregates such as have been described for intrabodies like scFvs⁵.

We then investigated the ability of the GFP-chromobody to access and bind its epitope in different subcellular compartments and structures in living cells. As a typical epitope in the cytoplasm, we used GFP-β-actin (**Supplementary Fig. 3** online), which is incorporated into growing actin filaments and allows direct visualization of actin-containing structures⁶. We cotransfected HeLa cells with GFP-β-actin and GFP-chromobody expression vectors and analyzed them by live cell microscopy (**Supplementary Methods**). A representative confocal image of a double-transfected cell showed green and red fluorescence at the cytoskeleton (**Fig. 1b**), indicative of correct incorporation of GFP-β-actin into the actin filaments and efficient recognition by the GFP-chromobody. The efficient epitope binding of the α-GFP V_HH domain of the chromobody indicated that its intrinsic stability ($\Delta G = 30 \text{ kJ/mol}$)⁷ was sufficient for proper folding and intracellular function.

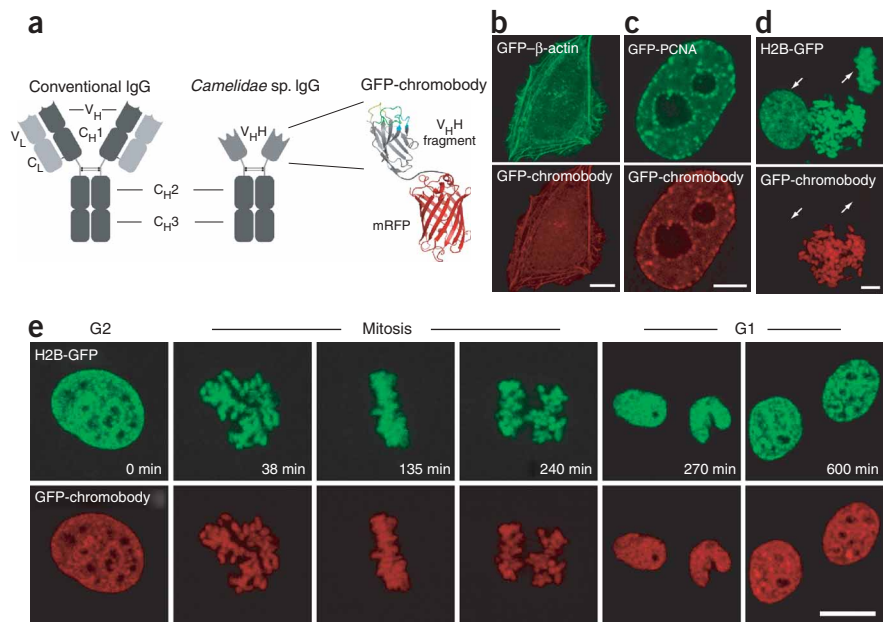
We next chose three well-characterized GFP fusions to test antigen binding in different nuclear structures, by cotransfecting HeLa cells with GFP fusion proteins and the GFP-chromobody. We used a GFP-lamin B1 fusion that assembles into nuclear lamina of mammalian cells⁸ (data not shown), a GFP fusion of proliferating cell nuclear antigen (PCNA) as an example of a nucleoplasmic epitope⁹ (**Fig. 1c**), and an epitope embedded in chromatin using a HeLa cell line stably expressing a histone H2B-GFP fusion that assembles into nucleosomes¹⁰ (**Fig. 1d**). In all experiments, the GFP-chromobody colocalized with the GFP fusion proteins. Moreover, the images of the untransfected cells clearly showed that no

¹Ludwig Maximilians University Munich, Department of Biology II, Grosshaderner Str. 2, 82152 Planegg-Martinsried, Germany. ²Institute of Gene Biology of the Russian Academy of Sciences, Vavilov Str. 34/5, 119334 Moscow, Russia. ³Max Delbrueck Center for Molecular Medicine, Robert-Roessle Str. 10, 13125 Berlin, Germany.

⁴Vrije Universiteit Brussel, Laboratory of Cellular and Molecular Immunology, Pleinlaan 2, 1050 Brussels, Belgium. ⁵These authors contributed equally to this work. Correspondence should be addressed to H.L. (h.leonhardt@lmu.de).

Figure 1 | Generation and characterization of a GFP-binding chromobody. (a) Schematic outline of a conventional IgG antibody in comparison with a *Camelidae*-derived heavy-chain IgG antibody and a generic chromobody. The putative structure of the chromobody, based on the known crystal structures of a V_HH and mRFP, is shown at right, with the three antigen-binding loops in yellow, cyan and green. (b–d) Targeting of the GFP-chromobody to GFP fusion proteins localizing in different cellular compartments and structures in HeLa cells.

(b) GFP-chromobodies colocalize with GFP-β-actin on cytoskeletal actin filaments. (c) GFP-chromobodies bind to GFP-PCNA at replication foci; a cell in mid S phase is shown. (d) GFP-chromobodies bind to the histone H2B-GFP incorporated into chromatin. The cell transfected with the GFP-chromobody was in prometaphase and condensed chromosomes are visible. Untransfected cells in metaphase and interphase (marked by arrows) that did not express the chromobody indicate that no unspecific bleed-through of green fluorescence occurred under these experimental conditions. Confocal mid-sections (b–c) and z-projection (d) of living cells are shown. Scale bars, 5 μm. (e) Tracing of a chromatin protein throughout mitosis. Time-lapse imaging of a HeLa cell stably expressing histone H2B-GFP transfected with GFP-chromobody. Selected frames from this time series are shown. At the time imaging was started (0 h), this cell was in late G2 phase. Scale bars, 10 μm. (See also **Supplementary Video 1.**)



fluorescence bleed-through occurred under these experimental conditions (**Fig. 1d**; see arrows). These results demonstrated that the GFP-chromobody efficiently recognizes and binds its epitope in different structures and subcellular compartments.

We then tested the ability of the GFP-chromobody to trace its antigen throughout the cell cycle, again using H2B-GFP and GFP-PCNA. Time-lapse microscopy of transfected HeLa cells showed that colocalization of the GFP-chromobody with H2B-GFP persisted through various chromatin condensation states during mitosis (**Fig. 1e** and **Supplementary Video 1** online). GFP-PCNA constitutes a special challenge to live cell microscopy because it is an essential component of the replication machinery that concentrates at replication foci in S phase and shows a diffuse

pattern in G1 and G2 (ref. 9). We followed the subcellular distribution of GFP-PCNA and GFP-chromobody from early S until G2 phase by taking confocal three-dimensional image stacks every 20 min (**Supplementary Fig. 4** and **Supplementary Video 2** online). Both GFP-PCNA and the chromobody showed typical punctate patterns followed by a disperse distribution, indicating progression through S phase and transition to G2 phase. These time-lapse analyses show that chromobodies can trace integral chromatin components such as H2B as well as essential components of the replication machinery without major impact on cell cycle progression and viability.

To test whether chromobodies can also recognize and trace endogenous epitopes, we generated chromobodies against cytoplasmic and nuclear antigens. We selected V_HHs that specifically bind to cytokeratin-8 and lamin Dm0, fused them to mRFP and tested the subcellular distribution of the resulting chromobodies in a variety of higher eukaryotic cells. The cytokeratin-8-chromobody highlighted cytoplasmic filaments, indicative of binding to the endogenous cytokeratin structures (**Fig. 2a**). In contrast, the lamin-chromobody was localized at the nuclear rim in *Drosophila melanogaster* S2 and HeLa cells (**Fig. 2b**), indicating efficient recognition of endogenous lamina lining the nucleus in cells derived from two organisms as different as insect and humans.

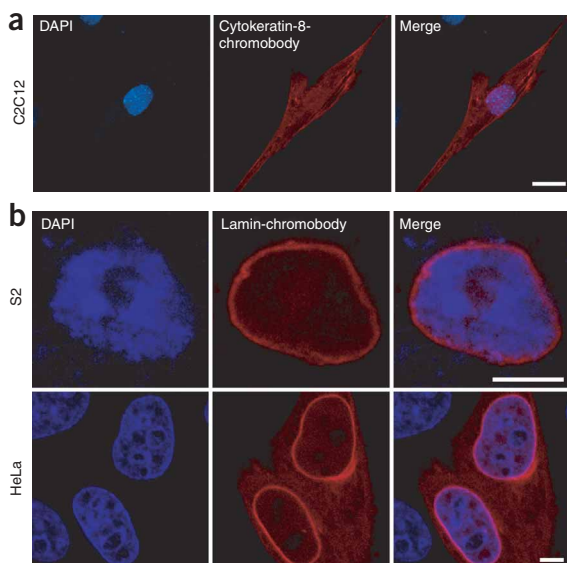


Figure 2 | Recognition of subcellular structures by chromobodies raised against endogenous epitopes. (a) Confocal microscopy images of mouse myoblast cells (C2C12) fixed and stained with 4',6-diamino-2-phenylindole dihydrochloride (DAPI) 24 h after transfection with the cytokeratin-8-chromobody. The red fluorescence on cytoplasmic filaments indicates the recognition of cytokeratin fibers. Scale bar, 20 μm. (b) Confocal microscopy images of *D. melanogaster* S2 cells and human HeLa cells fixed and stained with DAPI 24 h and 48 h after transfection with the lamin-chromobody expression plasmid. The red fluorescence of the chromobody highlights a nuclear rim structure that is characteristic of the nuclear lamina. Scale bars, 5 μm.

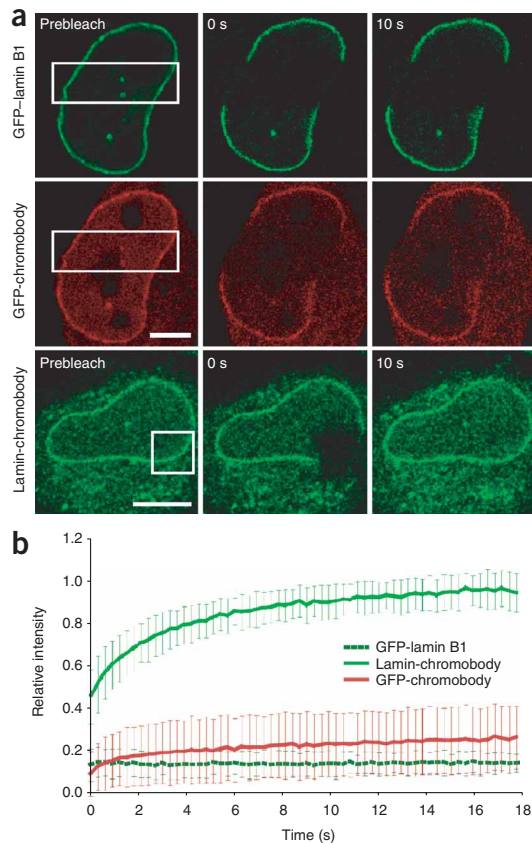


Figure 3 | *In vivo* binding properties of various chromobodies analyzed by FRAP. **(a)** FRAP of GFP-lamin B1 (top; green) and GFP-chromobody (middle; red) coexpressed in a HeLa cell. Photobleaching of a small region (box) resulted in no recovery of GFP-lamin B1 and only slow recovery of GFP-chromobody during the observation period. FRAP of lamin-chromobody (bottom; green) expressed in a different HeLa cell revealed a quick recovery of lamin chromobody within less than 20 s. Scale bars, 5 μ m. **(b)** Quantitative evaluation of FRAP data showing mean curves, $n = 10$. Error bars, s.d.

deliberately target catalytic or regulatory sites for functional studies. The small size and compact structure of the antigen-binding domain of the chromobodies supports their intracellular stability and should allow access to epitopes that are not reached by larger, conventional antibodies (**Supplementary Fig. 1**). This smaller size could, however, limit the maximally possible binding interface and strength of chromobodies.

The single $V_{\text{H}}\text{H}$ domain required for chromobodies can be amplified in one step from bulk lymphocyte mRNA to generate libraries from naive or immunized animals for rapid selection of specific binders^{13,14}. Thus in generating chromobodies one can take advantage of the affinity maturation occurring during the immunization process, which involves somatic mutations and *in vivo* selection of high-affinity binders. By comparison, Fab and scFv molecules require two matching fragments from heavy and light chains (**Supplementary Fig. 1**), which are usually obtained from monoclonal cell lines. The alpacas used in this study are the least demanding of all *Camelidae* and alpaca immunization is readily available in most countries. The availability of $V_{\text{H}}\text{H}$ libraries, combined with continually improving maturation and selection techniques, will further facilitate the generation of new chromobodies. We anticipate that chromobodies and related tools will expand the possibilities of live cell microscopy and make entirely new functional studies possible, as potentially any antigenic cellular structure can be targeted and traced in living cells.

Note: Supplementary information is available on the Nature Methods website.

ACKNOWLEDGMENTS

We thank R.Y. Tsien, J. Ellenberg and K.F. Sullivan for providing expression vectors and cell lines, and J. Fünér for the alpaca immunization. This work was supported by grants from the Deutsche Forschungsgemeinschaft to M.C.C. and H.L.

COMPETING INTERESTS STATEMENT

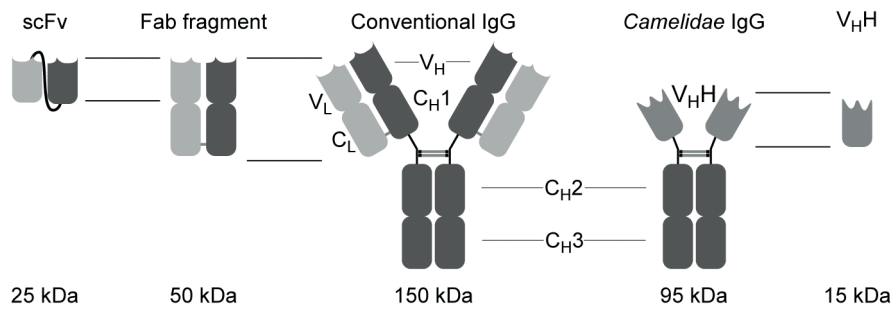
The authors declare that they have no competing financial interests.

Published online at <http://www.nature.com/naturemethods/>
Reprints and permissions information is available online at
<http://npg.nature.com/reprintsandpermissions/>

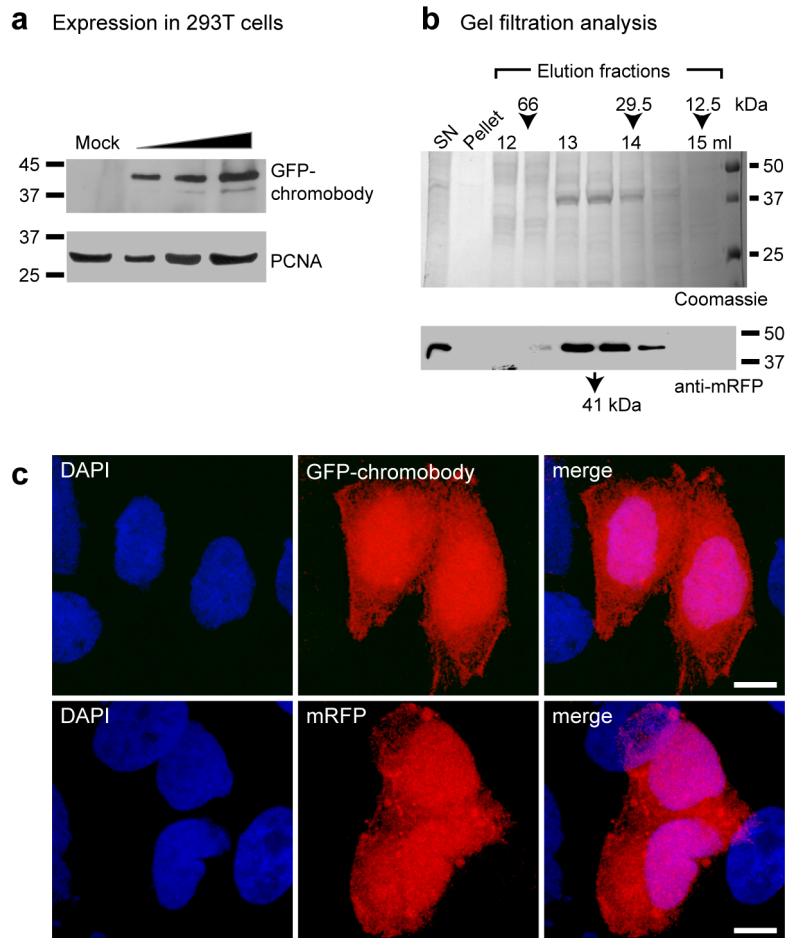
Finally, we investigated the antigen-binding dynamics of chromobodies by measuring the fluorescence recovery after photobleaching (FRAP). We compared the binding of the lamin-chromobody and the GFP-chromobody with the recovery rate of the GFP-lamin B1 fusion, which is a stable component of the nuclear lamina with practically no turnover¹¹. As expected, GFP-lamin B1 showed no detectable recovery after photobleaching and the GFP-chromobody showed very little recovery of fluorescence at the nuclear lamina, indicating high-affinity binding of its epitope (**Fig. 3a,b**). In contrast, the lamin-chromobody showed a quick recovery of fluorescence, with a half-time ($t_{1/2}$) of ~ 1.9 s, indicating transient lamin binding with rapid turnover (**Fig. 3a,b**). These results demonstrate that chromobodies can be raised with different binding affinities and that even transient binding can be sufficient for visualization of cellular structures. Transient binding of chromobodies is likely to be less harmful to cells than permanent fusion with a fluorescent protein.

Chromobodies combine the wide target range of antibodies with the live cell capabilities of fluorescent protein fusions and thus potentially allow tracing of any cellular epitope, including endogenous proteins, their post-translational modifications and various conformational states as well as non-protein components in living cells. Recent work describing the detection of a specific protein conformation with scFvs¹² exemplifies new applications made possible with recombinant antibody technologies. As chromobodies can be selected against the entire antigen surface and their affinities adjusted by mutagenesis, it should be possible either to minimize functional interference for antigen tracing or to

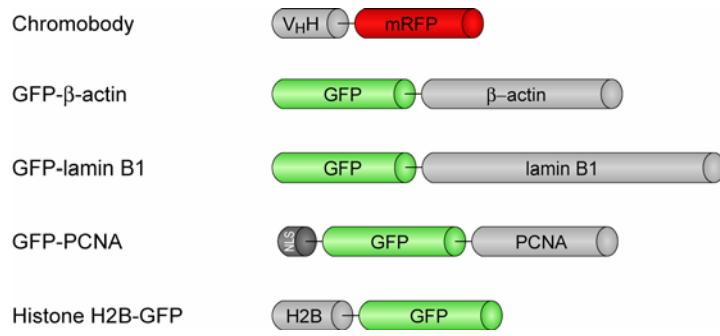
1. Chalfie, M. *et al. Science* **263**, 802–805 (1994).
2. Tsien, R.Y. *Annu. Rev. Biochem.* **67**, 509–544 (1998).
3. Hamers-Casterman, C. *et al. Nature* **363**, 446–448 (1993).
4. Muyldermans, S. *J. Biotechnol.* **74**, 277–302 (2001).
5. Cardinale, A., Filesi, I., Mattei, S. & Biocca, S. *Methods* **34**, 171–178 (2004).
6. Westphal, M. *et al. Curr. Biol.* **7**, 176–183 (1997).
7. Saerens, D. *et al. J. Mol. Biol.* **352**, 597–607 (2005).
8. Daigle, N. *et al. J. Cell Biol.* **154**, 71–84 (2001).
9. Leonhardt, H. *et al. J. Cell Biol.* **149**, 271–280 (2000).
10. Kanda, T., Sullivan, K.F. & Wahl, G.M. *Curr. Biol.* **8**, 377–385 (1998).
11. Moir, R.D., Yoon, M., Khuon, S. & Goldman, R.D. *J. Cell Biol.* **151**, 1155–1168 (2000).
12. Nizak, C. *et al. Science* **300**, 984–987 (2003).
13. Jobling, S.A. *et al. Nat. Biotechnol.* **21**, 77–80 (2003).
14. Arbabi Ghahroudi, M. *et al. FEBS Lett.* **414**, 521–526 (1997).



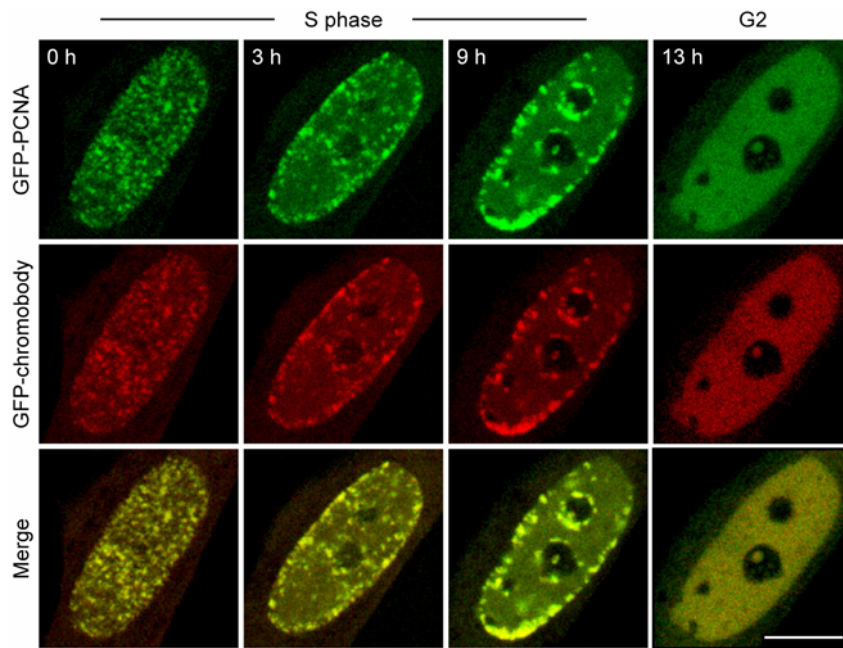
Supplementary Figure 1. Schematic comparison of a conventional IgG and a Heavy-chain IgG from *Camelidae* and various antigen-binding fragments derived thereof. The antigen binding domains of a conventional antibody are Fabs (fragment antigen binding) and Fv fragments. The Fab fragments are the antigen binding domains of an antibody molecule, containing $V_H + C_{H1}$ and $C_L + V_L$. The C_L and C_{H1} are connected through an intrachain disulfide bond. The molecular weight of the heterodimer is around 50 kDa. Fab fragments can be prepared by papain digestions of whole antibodies. Normally, recombinant Fv fragments composed of both the variable heavy chain (V_H) and the variable light chain (V_L) are unstable since the non-covalently associated domains tend to dissociate. To remediate this unstable behavior, the V_H and V_L domains are tethered by hydrophilic and flexible peptide linker $(Gly_4Ser)_3$. Such scFv (single chain Fv fragments) are the minimal fragments that still contain the whole antigen-binding site of an IgG antibody. Heavy-chain IgGs from *Camelidae* are only composed of the heavy chains and lack the light chain completely. Also the first constant region (C_{H1}) is missing in these Heavy-chain antibodies (spliced out during mRNA processing due to loss of a splice consensus signal). The antigen-binding domain, referred to as V_{HH} (15 kDa) to distinguish it from a V_H of the conventional IgG, contains some key mutations that prevent all pairing to possible V_L domains. The isolated V_{HH} s are the smallest available intact antigen-binding fragment that can be cloned after PCR amplification of one single exon, whereas a scFv requires separate V_H and V_L amplification and subsequent joining. The affinities of V_{HH} s to their cognate antigen are in the nanomolar range and comparable with those of Fab and scFv fragments. In contrast to other fragments, V_{HH} s are highly soluble and stable under challenging conditions as high salts, detergents or at elevated temperatures.



Supplementary Figure 2. The GFP-chromobody is present as a stable monomeric protein in mammalian cells. **(a)** Total cell extracts of GFP-chromobody expressing 293T cells or mock treated cells were prepared 72 h after transfection and were analyzed by SDS-PAGE and immunostaining. Lane 1: 30 μ g of protein extract of mock transfected cells; lane 2-4: 10, 20 and 30 μ g of protein extract of GFP-chromobody expressing cells. The predicted size of the chimeric protein is 41 kDa (upper panel). As a loading control, the blot was reincubated with an antibody against PCNA (lower panel). **(b)** Gel filtration analysis of extracts of mammalian cells expressing the chromobody. The GFP-chromobody elutes from the column in peak fractions corresponding to an apparent molecular mass of \sim 40 kDa. Arrowheads indicate the elution of calibration standards. **(c)** Expression of the GFP-chromobody in HeLa cells in the absence of any antigen shows a dispersed distribution of the protein throughout the cytoplasm and the nucleus (upper panel), which is comparable to the distribution of non-fused mRFP in the same cell type (lower panel).



Supplementary Figure 3. Schematic representation of the fusion proteins used in this study.



Supplementary Figure 4. Antigen tracing with chromobodies. Tracing of a component of the replication machinery throughout S phase until G2. Time lapse imaging of cotransfected HeLa cell expressing GFP-PCNA and GFP-chromobody. Selected frames from this series are shown. At the start of imaging (0 h) the cell was in early to mid S phase. Scale bar, 10 μ m. (See also **Supplementary Video 2.**)

Supplementary Methods

GFP expression, purification and llama immunization. *Escherichia coli* BL21DE3 cells were transformed with pRSETB-GFPS65T¹ (kindly provided by Roger Y. Tsien, UCSD) and overexpressed (His₆)-tagged GFPS65T was purified using ion-metal affinity chromatography according to the manufacturer's instructions (Talon, Clontech, CA, USA). One llama alpaca (*Lama pacos*) was immunized with recombinant purified GFP in Gerbu adjuvant according to the following scheme: day 0, 250 µg GFP; days 7, 14, 21, 28 and 35, 100 µg GFP; day 42, a bleed of 150 ml was collected.

V_HH library construction and selection of the antigen specific V_HH. Heparinized blood (36 ml) was diluted with prewarmed RPMI and layered on LymphoprepTM (AXIS-Shield, Oslo, Norway) to purify the PBL cells according to the manufacturer's instructions. A total of 2×10⁷ PBL cells were isolated and stored at -80°C in aliquots of 6×10⁶ cells. The mRNA was extracted from 6×10⁶ lymphocytes and cDNA was synthesized with SuperscriptII RNaseH⁻ reverse transcriptase (Invitrogen, CA, USA) using an oligo-dT primer. The first PCR on the cDNA template was performed using CALL001 (5'-GTC CTG GCT GCT CTT CTA CA AGG-3') and CALL002 (5'-GGT ACG TGC TGT TGA ACT GTT CC-3') primers annealing at the leader sequence and at the CH2 exon of the heavy chains of all llama IgGs, respectively. The PCR products lacking the CH1 sequences (i.e. fragments with sizes between 650 -750 bp) were purified from an agarose gel using QIAquick PCR gel extraction kit (Qiagen-GmbH, Hilden, Germany). A nested PCR was done with an equimolar mixture of primers SM017 and SM018 (5'-CCA GCC GGC CAT GGC TCA GGT GCA GCT GGT GGA GTC TGG-3' and 5'-CCA GCC GGC CAT GGC TGA TGT GCA GCT GGT GGA GTC TGG-3', respectively) and CALL002 primer, and the PCR product repurified from agarose gel as described before. The V_HH genes were finally re-amplified with primers A4short (5'-CAT GCC ATG ACT CGC GGC CAC GCC GGC CAT GGC-3') and 38 (5'-

GGA CTA GTG CGG CCG CTG GAG ACG GTG ACC TGG GT-3') and digested with restriction enzymes NcoI and NotI to obtain sticky DNA ends. The fragment was purified with QIAquick, ligated into pHEN4 vector² cut with the same enzymes and the ligation mixture used to transform *Escherichia coli* TG1 cells. After overnight growth on LB/ampicillin plates, the bacterial colonies were scraped from the plates in LB, washed in the same medium and stored in LB/15% glycerol at -80°C until further use. A V_HH library of 10⁶ individual clones was obtained in *Escherichia coli* TG1 cells. A representative aliquot of this library was used to inoculate LB/ampicillin until cells reached the exponential growth phase before infection with M13K07 helper phages to display the cloned V_HH at the tip of the virions. The phage displayed V_HH library was panned for the presence of α-GFP V_HH on solid phase coated GFP (0.1 μg GFP / 100 μl per well) for three consecutive rounds. After the third round of selection, individual colonies were picked and expression of their soluble periplasmic protein was induced with 1 mM IPTG. The recombinant V_HH extracted from the periplasm was tested for antigen recognition in an ELISA. For further investigation of the binding specificity of the α-GFP V_HH, a C-terminal histidine (His₆)-tagged bacterial expression plasmid was constructed and the soluble recombinant antibody fragment was purified from *Escherichia coli* WK6 cells. The α-GFP V_HH was highly expressed and yielded 0.7 - 1 mg of soluble V_HH per 200 ml of IPTG-induced bacterial culture. The cytokeratin-8 and *Drosophila* lamin Dm0 specific V_HH's were obtained from an immunized camel using a similar protocol as for retrieving the α-GFP V_HH.

Expression and purification of the single-domain antibody fragment. The V_HH gene of the clone that scored positive in ELISA (α-GFP V_HH) was recloned into the pHEN6 expression vector and used to transform *Escherichia coli* WK6 cells. Large scale production and purification followed the protocol described by Saerens et al.³

Generation of chromobodies. The plasmid construct encoding a translational fusion of α -GFP V_HH and mRFP was derived by PCR amplification of the α -GFP V_HH coding region with primers gfp4#F (5'-GGG GGC TCG AGC CGG CCA TGG CCG ATG TGC AG-3') and gfp4#RC (5'-GGG GGA ATT CCT TGA GGA GAC GGT GAC-3'). In the case of the α -lamin-V_HH and the α -cytokeratin V_HH the corresponding cDNA, was amplified by PCR with primers V_HH (BglII)#F (5'-GGG GAG ATC TCC GGC CAT GGC TCA GGT GCA G-3') and gfp4#RC (5'-GGG GGA ATT CCT TGA GGA GAC GGT GAC-3'). The PCR product was purified as described and digested with restriction enzymes XhoI and EcoRI or BglII and EcoRI and ligated into a modified pEYFP-N1 vector (Clontech, CA, USA) where the YFP sequence had been replaced by the mRFP1 coding region ⁴.

Affinity measurements. Affinity measurements were done by addition of different concentrations of GFP, ranging from 500 nM to 7.5 nM, to purified his-tailed α -GFP V_HH attached on a nickel-nitrilo triacetic acid biochip (Biacore International AB, Uppsala, Sweden) according to the manufacturer's description. The kinetic binding parameters k_{on} , k_{off} and K_d were determined with the BIAevaluation software (version 3.0).

Mammalian expression constructs. The plasmid constructs encoding translational fusions of GFP were as follows: GFP- β -actin (Clontech, CA, USA), GFP-lamin B1 ⁵, GFP-PCNA ⁶.

Mammalian cell culture and transfection. 293T cells, HeLa cells, HeLa cells stably expressing H2B-GFP ⁷ and C2C12 mouse myoblasts, were cultured in DMEM supplemented with 10% FCS and 20% FCS for C2C12. 293T cells were transfected with plasmid DNA using TransFectin™ reagent (Bio-Rad Laboratories, Hercules, CA, USA) according to the manufacturer's guidelines and incubated overnight, 48 h or 72 h respectively before performing the immunoblots. For microscopy HeLa cells were grown to 50-70 % confluence

either on 18×18 mm glass coverslips, 40 mm round glass coverslips, in μ -Slides (ibidi®, Munich, Germany) or on Lab-Tek™ Chambered Coverglass (Nunc-GmbH, Wiesbaden, Germany) and were transfected with the indicated expression constructs using Polyplus transfection reagent jetPEI™ (BIOMOL GmbH, Hamburg, Germany) according to the manufacturer's instructions. After 4-6 hours the transfection medium was changed to fresh culture medium and cells were then incubated for another 24 hours before performing live cell microscopy or fixation with 3.7 % formaldehyde in PBS for 10 min at room temperature. Fixed cells were permeabilized with 0.2 % Triton X-100 in PBS for 3 min, counterstained with DAPI and mounted in Vectashield (Vector Laboratories, CA, USA).

Drosophila cell culture and transfection. Schneider S2 cells were cultured in Schneider's Drosophila Medium containing 10% heat inactivated FBS at 26°C. Cells were transfected using Effectene™ reagent (QIAGEN Inc, Valenica, CA, USA) according to the manufacturer's guidelines and incubated for 48 hours at 26°C. After resuspension S2 cells were seeded on 18×18 mm glass coverslips. After 2 hours cells were fixed with 2.5% formaldehyde in PBS for 7 min on ice. Fixed cells were permeabilized with 0.2 % Triton X-100 in PBS for 3 min, counterstained with DAPI and mounted in Vectashield (Vector Laboratories, CA, USA).

Western blot analysis. Increasing protein amounts of total cell extracts of 293T cells either mock transfected or expressing the GFP-chromobody were separated on a 12% SDS-PAGE and then electrophoretically transferred to nitrocellulose membrane (Bio-Rad Laboratories, CA, USA). The membrane was blocked with 3% milk in PBS and incubated overnight at 4°C with an mRFP rabbit polyclonal antibody. After washing with PBS containing 0.1% Tween-20, the blots were incubated with rabbit IgG antibody conjugated with horseradish peroxidase. Immunoreactive bands were visualized with ECL plus Western Blot Detection Kit

(Amersham Biosciences, NJ, USA). As a loading control, membranes were reprobed with PCNA antibody.

Gel filtration. Extracts from 293T cells expressing the GFP-chromobody were subjected to gel filtration analysis. Briefly, 1×10^7 cells were homogenized in 500 μ l lysis buffer (20 mM Tris/HCl pH 7.5, 150 mM NaCl, 0.5 mM EDTA, 2 mM PMSF, 0.5% NP40). After a centrifugation step (10 min, 20,000 \times g, 4°C) the clear supernatant was loaded on a Superose-12 column (Amersham Pharmacia Biotech, NJ, USA) and chromatographed at a flowrate of 0.4 ml/min in column buffer (20 mM Tris/HCl pH 7.5, 150 mM NaCl, 0.5 mM EDTA). Fractions (500 μ l each) were analyzed by SDS-PAGE and proteins were either stained with Coomassie Brilliant Blue R-250 or probed further by western blotting followed by incubation with an antibody against mRFP as described above. As calibration standards bovine serum albumin (66 kDa), carbonic anhydrase (29.5 kDa) and cytochrome c (12.5 kDa) were used.

Microscopy. Live or fixed cells expressing fluorescent proteins were analyzed using a Leica TCS SP2 AOBS confocal microscope equipped with a 63 \times /1.4 NA Plan-Apochromat oil immersion objective. Fluorophores were excited with a 405 nm Diode laser, a 488 nm Ar laser, a 561 nm Diode-Pumped Solid-State (DPSS) laser. Confocal image stacks of living or fixed cells were typically recorded with a frame size of 512 \times 512 pixels, a pixel size of 70-160 nm, a z step size of 280 nm and the pinhole opened to 1 Airy unit. A maximum intensity projection of several mid z-sections was then performed using ImageJ (Version 1.34, <http://rsb.info.nih.gov/ij/>). For long term live cell observation 40 mm diameter glass coverslips were mounted in a FCS2 live-cell chamber (Bioptechs, Butler, PA, USA) and maintained at 37°C. Light optical sections were acquired with a Zeiss LSM410 confocal laser scanning microscope using the 488 nm Ar laser line and the 543 nm HeNe laser line. Three mid z-sections at 1 μ m intervals and the pinhole opened to 2 Airy Units were taken at

indicated time intervals. Cells were followed up to 12 hours. Focus drift over time was compensated with a macro, which uses the reflection at the coverslip to medium interface as reference. After image acquisition, a projection of the three z-sections was performed from each time point. For colocalization analysis the “colocalization-finder” plug-in (Version 1.1) for ImageJ written by C. Laummonerie was used. For FRAP analysis, a region of interest was selected and photobleached by an intense laser beam (laser lines 458 nm, 476 nm, 488 nm, 496 nm, 514 nm and 561 nm set to maximum power at 100% transmission) for 300 ms. Before and after bleaching, confocal image series were recorded at 300 ms time intervals (typically 5 prebleach and 60 postbleach frames) with the pinhole opened to 1.5 Airy units. Mean fluorescence intensities of the bleached region were corrected for background and for total nuclear loss of fluorescence over the time course and normalized to the mean of the last 4 prebleach values. For the quantitative evaluation of FRAP experiments, data of 10 nuclei were averaged and the mean curve as well as the standard deviation was calculated.

References

1. Heim, R., Cubitt, A.B. & Tsien, R.Y. Improved green fluorescence. *Nature* **373**, 663-664 (1995).
2. Arbabi Ghahroudi, M., Desmyter, A., Wyns, L., Hamers, R. & Muyldermans, S. Selection and identification of single domain antibody fragments from camel heavy-chain antibodies. *FEBS Lett.* **414**, 521-526 (1997).
3. Saerens, D. *et al.* Identification of a universal VHH framework to graft non-canonical antigen-binding loops of camel single-domain antibodies. *J Mol Biol* **352**, 597-607 (2005).
4. Campbell, R.E. *et al.* A monomeric red fluorescent protein. *Proc. Natl Acad. Sci. U S A* **99**, 7877-7882 (2002).
5. Daigle, N. *et al.* Nuclear pore complexes form immobile networks and have a very low turnover in live mammalian cells. *J. Cell. Biol.* **154**, 71-84 (2001).
6. Leonhardt, H. *et al.* Dynamics of DNA replication factories in living cells. *J. Cell. Biol.* **149**, 271-280 (2000).
7. Kanda, T., Sullivan, K.F. & Wahl, G.M. Histone-GFP fusion protein enables sensitive analysis of chromosome dynamics in living mammalian cells. *Curr. Biol.* **8**, 377-385 (1998).